

Nitrogen Atom Transfer from Iron(IV) Nitrido Complexes: A Dual-Nature Transition State for Atom Transfer

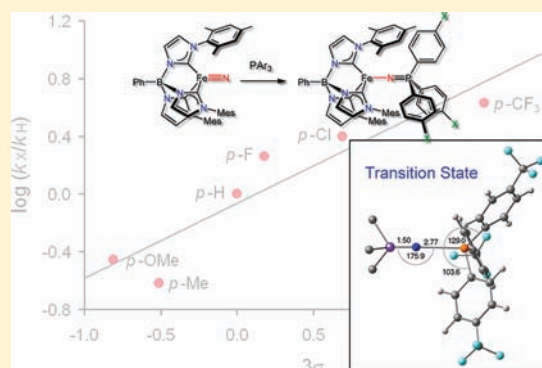
Jeremiah J. Scepaniak,[†] Charles G. Margarit,[†] Jeremy N. Harvey,^{*,‡} and Jeremy M. Smith^{*,†}

[†]Department of Chemistry and Biochemistry, New Mexico State University, MSC 3C, Las Cruces New Mexico 88003, United States

[‡]Centre for Computational Chemistry, University of Bristol, Bristol BS8 1TS, United Kingdom

S Supporting Information

ABSTRACT: The mechanism of nitrogen atom transfer from four-coordinate tris(carbene)borate iron(IV) nitrido complexes to phosphines and phosphites has been investigated. In the absence of limiting steric effects, the rate of nitrogen atom transfer to phosphines increases with decreasing phosphine σ -basicity. This trend has been quantified by a Hammett study with *para*-substituted triarylphosphines, and is contrary to the expectations of an electrophilic nitrido ligand. On the basis of electronic structure calculations, a dual-nature transition state for nitrogen atom transfer is proposed, in which a key interaction involves the transfer of electron density from the nitrido highest occupied molecular orbital (HOMO) to the phosphine lowest unoccupied molecular orbital (LUMO). Compared to analogous atom transfer reactions from a 5d metal, these results show how the electronic plasticity of a 3d metal results in rapid atom transfer from pseudotetrahedral late metal complexes.



INTRODUCTION

The transition metal-catalyzed transfer of atoms from small molecules to larger substrates is an atom-economical method for introducing functionality. Both synthetic and biological atom transfer catalysts are known.¹ For example, cytochrome P450 and its isozymes catalyze the oxidation of multiple organic substrates using O₂ as the oxygen atom source. An iron(IV) oxo intermediate is believed to be the active oxidant (Figure 1).² Similar oxygen atom transfer from transition metal oxo intermediates has also been implicated as a key mechanistic step in the catalytic cycles of other metalloenzymes, for example, oxygen-evolving chlorite dismutase,³ nonheme dioxygenases,^{4,5} and oxotransferases.^{1,6}

The mechanisms of oxygen atom transfer from metal oxo complexes to substrates have been extensively investigated. The rate of oxygen atom transfer can often be rationalized in terms of thermodynamic driving forces,⁷ although other factors may be important. For example, it has been found that oxygen atom self-exchange is subject to similar considerations as outer sphere electron transfer, with reorganizational energies being key to determining the activation barrier for atom transfer.⁸ Changes in metal spin state may also play a critical role in oxygen atom transfer, as shown for group 5 complexes in 3-fold symmetry, where the spin state energetics dictate the geometry of the transition state (TS).⁹

Analogously to transition metal oxos, nitrido complexes have the potential for mediating nitrogen atom transfer to organic substrates, most notably using N₂ as the nitrogen atom source.¹⁰ Despite this promise, transition metal-mediated nitrogen atom transfer is not nearly as well developed as oxygen atom transfer.

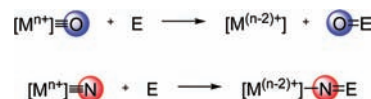


Figure 1. Two electron atom transfer from metal oxo and nitrido complexes.

Three electron reactions involving the complete transfer of nitrogen atoms between two metal complexes are known,¹¹ but few nonmetallic substrates are able to participate in three electron reactions. Nitrido ligands can also participate in two electron nitrogen atom transfer reactions, resulting in the formation of new ligands (Figure 1). The substrate scope for these incomplete atom transfer reactions appears to be similar to that for oxygen atom transfer. Thus, for example, two electron nitrogen atom transfer reactions to nucleophiles such as phosphines,¹² isonitriles,¹³ carbenes,¹⁴ and alkenes¹⁵ have been reported, leading to the formation of phosphoraniminato, carbo-diimido, ketimido, and aziridine ligands, respectively. An interesting twist on this reactivity is the [4 + 1] cycloaddition of nitrido ligands with cyclohexadienes to yield dihydropyrrolides.¹⁶

A priori, it may be expected that the factors that influence two electron oxygen atom transfer will similarly impact nitrogen atom transfer. This expectation appears to be true for nitrogen atom self-exchange reactions, first investigated in metal porphyrins¹⁷ and subsequently in analogous salen¹⁸ and corrole¹⁹ complexes.

Received: June 2, 2011

Published: September 08, 2011

Chart 1

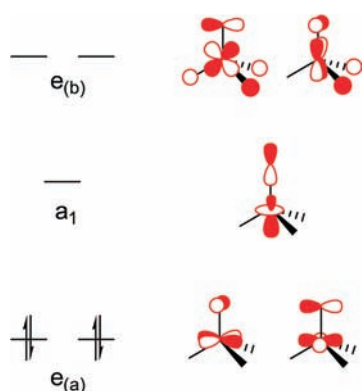
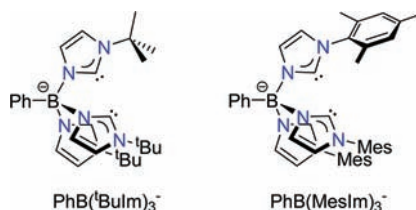


Figure 2. Qualitative frontier orbital diagram for tris(carbene)borate iron(IV) nitrido complexes.

In these reactions, the driving force for atom transfer is determined by the relative stability of higher oxidation states. The insights from these studies have inspired intermetallic nitrogen atom transfer as a protocol for the synthesis of new nitrido complexes.²⁰ There are few mechanistic studies on the transfer of nitrogen atoms to nonmetallic substrates,²¹ even though these reactions have been known since the early 1970s.²² It has generally been assumed that nitrogen atom transfer involves nucleophilic attack of the substrate on the nitrido ligand,²³ analogous to oxygen atom transfer.

We have previously reported terminal iron(IV) nitrido complexes supported by bulky tris(carbene)borate ligands (Chart 1). Our initial report on the synthesis and electronic structure of the complex $\text{PhB}(\text{tBuIm})_3\text{Fe}\equiv\text{N}$ (**1**) revealed a low-lying lowest unoccupied molecular orbital (LUMO) that is stabilized by iron spd mixing (Figure 2).²⁴ The degenerate highest occupied molecular orbital (HOMO) has mixed N lone pair and iron character: the σ lone pair on nitrogen is much lower in energy. The electronic structure suggested that the nitrido ligand should be electrophilic, and consistent with this expectation, the complex reacted cleanly with PPh_3 to yield the iron(II) complex $\text{PhB}(\text{tBuIm})_3\text{Fe}-\text{N}=\text{PPh}_3$ (**2**).²⁵ Unfortunately, an attempt to evaluate the electrophilicity of the nitrido ligand by a Hammett study involving a series of *para*-substituted triarylphosphines was unsuccessful, and no correlation between the relative rate of nitrogen atom transfer and any Hammett parameter was observed. This was tentatively attributed to the overwhelming impact of steric interactions between the substrate and the bulky *tert*-butyl substituents of the supporting tris(carbene)borate ligand.

In this paper we report further mechanistic studies on nitrogen atom transfer from iron(IV) nitrido complexes to phosphorus(III) nucleophiles. Since the topology of the supporting tris(carbene)borate ligand in $\text{PhB}(\text{MesIm})_3\text{Fe}\equiv\text{N}^{26}$ (**3**) makes the

$[\text{Fe}\equiv\text{N}]$ unit more accessible to the incoming substrate, we have been able to evaluate the electronic character of the transition state through a combination of experimental and computational methods. Although the nitrogen atom transfer reaction is spin forbidden, spin state changes do not play a role in the rate of reaction or its electronic selectivity. We find that nitrogen atom transfer involves a dual-nature transition state in which the nitrido ligand has both electrophilic and nucleophilic character.

EXPERIMENTAL SECTION

General Considerations. All manipulations were performed under a nitrogen atmosphere by standard Schlenk techniques or in an M. Braun Labmaster glovebox. The quality of the glovebox atmosphere was periodically checked with a toluene solution of “titanocene”.²⁷ Glassware was dried at 150 °C overnight. Diethyl ether, pentane, tetrahydrofuran, and toluene were purified by the Glass Contour solvent purification system. Deuterated benzene was dried first over CaH_2 , then over Na/benzophenone, before vacuum transfer into a storage container. Before use, aliquots of Et_2O , tetrahydrofuran (THF), and toluene were tested with a drop of sodium benzophenone ketyl in THF solution. Magnetic susceptibilities were determined in solution by the Evans’ method.²⁸ The iron(IV) nitrido complexes **1**²² and **3**²⁴ were prepared according to literature procedures. Phosphines were obtained from Strem Chemicals and Sigma-Aldrich, and were recrystallized twice from diethyl ether or THF prior to use. All other reagents were purchased from commercial vendors and used as received. ^1H NMR data were recorded on a Varian Unity 400 spectrometer (400 MHz) at 22 °C. All resonances in the ^1H NMR spectra are referenced to residual $\text{C}_6\text{D}_5\text{H}$ at δ 7.16 ppm.

Kinetic Measurements. *Reaction of $\text{PhB}(\text{tBuIm})_3\text{Fe}\equiv\text{N}$ (**1**) with Phosphines and Phosphites.* Tetrahydrofuran and toluene solutions of **1** and phosphine/phosphite were prepared in the glovebox at room temperature. All kinetics experiments used the initial concentration [**1**] = 0.565 mM. Reactions were monitored in 10 mm quartz cuvettes fitted with screwcaps using a temperature regulated CARY 100 Bio UV–visible spectrophotometer. The reactants were mixed inside the glovebox before being transferred to the spectrophotometer (thermally equilibrated at 26 °C). Reactions were monitored by measuring the decrease in absorbance at 480 nm. Pseudo first order rate constants were obtained from the slopes of plots of $\ln(A_t - A_\infty)$ versus time and were found to be linear over 2–3 half-lives. The observed pseudo first-order rate constants for the phosphines and phosphite were found to depend linearly on substrate concentration in the range 0.125 M–0.500 M.²⁹

*Reaction of $\text{PhB}(\text{MesIm})_3\text{Fe}\equiv\text{N}$ (**3**) with Triarylphosphines.* Toluene solutions of **3** and triarylphosphines were prepared in the glovebox at room temperature. All kinetics experiments used the initial concentration [**3**] = 0.468 mM while the initial phosphine concentrations were varied between 5.2 and 27.5 mM. The reagent solutions were loaded into syringes with fitted with locks and then attached to an Olis Rapid Scanning Monochromator stopflow spectrophotometer. Before each set of experiments the anhydrous environment was tested by monitoring the decay of **3** in the absence of substrate. The typical rate of decay was found to be 3 orders of magnitude slower than the slowest kinetic run. Reactions were monitored measuring the decrease in the absorbance at 500 nm. Pseudo first order rate constants were obtained using the Olis Globalworks software.³⁰ During the Eyring study the reagent solutions were allowed to thermally equilibrate for 10 min before kinetic measurements. Activation parameters were calculated by plotting $\ln(k_{\text{obs}}/T)$ vs $1/T$ over the range of 283–323 K.²⁷ Hammett studies were conducted using 5.3 mM solutions of *para*-substituted triarylphosphines.

Competition Experiments. The relative rates of nitrogen atom transfer from **3** to phosphine and phosphite substrates were determined by competition experiments and monitored by ^1H NMR spectroscopy. Thus, when the iron nitrido **3** (12.0 mg 17 μmol) is combined with a

solution of PPh_3 (5.0 mg, 19 μmol) and $\text{P}(\text{OPh})_3$ (45 μL , 170 μmol) in C_6D_6 (0.50 mL) the resulting ^1H NMR spectrum shows a 1:1 mixture of $\text{PhB}(\text{MesIm})_3\text{Fe}-\text{N}=\text{PPh}_3$ and $\text{PhB}(\text{MesIm})_3\text{Fe}-\text{N}=\text{P}(\text{OPh})_3$. Likewise, when **3** (14.0 mg, 20 μmol) is combined with a solution of PPh_3 (6.0 mg, 23 μmol) and $\text{P}(\text{OMe})_3$ (25 μL , 211 μmol) in C_6D_6 (0.50 mL) the resulting ^1H NMR spectrum also shows a 1:1 mixture of $\text{PhB}(\text{MesIm})_3\text{Fe}-\text{N}=\text{PPh}_3$ and $\text{PhB}(\text{MesIm})_3\text{Fe}-\text{N}=\text{P}(\text{OMe})_3$. Thus, nitrogen atom transfer from **3** to PPh_3 is an order of magnitude faster than to either $\text{P}(\text{OPh})_3$ or $\text{P}(\text{OMe})_3$. Finally, when a solution of **3** (10 mg, 14.0 μmol) in C_6D_6 (0.5 mL) is combined with a solution of $\text{P}(\text{OPh})_3$ (14.0 μmol) and $\text{P}(\text{OMe})_3$ (14.0 μmol) in C_6D_6 (0.5 mL) the resulting ^1H NMR spectrum shows a 3:1 mixture of $\text{PhB}(\text{MesIm})_3\text{Fe}-\text{N}=\text{P}(\text{OPh})_3$ and $\text{PhB}(\text{MesIm})_3\text{Fe}-\text{N}=\text{P}(\text{OMe})_3$.

Solution NMR Studies of Spin Crossover. The spin crossover behavior of **4** in solution was investigated by measuring the temperature dependence of the isotropic shifts in C_7D_8 between the temperatures of 198 and 378 K.³¹ The paramagnetic shift of the pure high spin complex were fit by taking an extended Curie law into account with different Curie constants (or spin densities) for the ground and excited states:

$$\delta_n^{\text{con}} = (F/T) \{W_1 C_{n1}^2 + W_2 C_{n2}^2 e^{-\Delta E/kT}\} / \{W_1 + W_2 e^{-\Delta E/kT}\}$$

where W_1 and W_2 are the weighting factors of the ground and excited states, C_{n1} and C_{n2} are the orbital coefficients for the ground and excited state, F is the Curie constant, ΔE is the energy difference between the ground and first excited state and k is the Boltzmann constant. Both ground and first excited states were assumed to exhibit a total spin $S = 2$. The data was fit using the TDF program written by Shokhirev and Walker.³² No difference between the observed and calculated isotropic shifts was observed, and thus **4** has a high spin configuration over this temperature range. Further details are provided in the Supporting Information.

Computational Details. The structures of the reactant in the singlet, triplet, and quintet states were optimized at the B3LYP level using the Jaguar program package.³³ The iron atom was described using the standard Los Alamos ECP together with the associated triple-zeta LACV3P basis as implemented in Jaguar.³⁰ All other atoms were described using the all-electron 6-31G(d) basis, with five d polarization functions. The phosphines PPh_3 , $\text{P}(p\text{-C}_6\text{H}_4\text{CF}_3)_3$ and $\text{P}(\text{OMe})_3$ as well as the product of the reaction with PPh_3 (in its singlet, triplet, and quintet states) were also studied at the same level of theory. The singlet TS for addition of the each of the three phosphines was also studied at this level. Single-point energies at the optimized geometries were computed using the Gaussian 03 program package,³⁴ and a larger basis set. This was composed of the Stuttgart ECP and associated triple- ζ basis set ('SDD' in Gaussian) for iron, augmented by two f polarization functions ($\zeta = 3.516$ and 0.871), of the 6-311+G(d) basis for the nitrogen, oxygen, and phosphorus atoms, and the 6-31G(d) basis for all other atoms. As well as vacuum calculations, single point energies in the presence of a continuum solvent model of toluene (IEF-PCM model, including all nonelectrostatic terms) were computed. Corrections for zero-point energy were obtained based on vibrational frequency calculations carried out for a model system (see details in the Supporting Information). Finally, dispersion-corrected B3LYP-D3 energies were obtained using the method and code of Grimme et al.³⁵ Unless mentioned otherwise, all energies are based on the larger basis B3LYP electronic energies, corrected with the model system zero-point energy. B3LYP-D3 and continuum solvent-corrected relative energies are also discussed in the text.

RESULTS

Reaction of Iron(IV) Nitrido Complexes with Phosphorus-(III) Nucleophiles. We have previously reported that addition of 1 equiv of PPh_3 to the iron(IV) nitrido complexes **1** and **3** results

Scheme 1

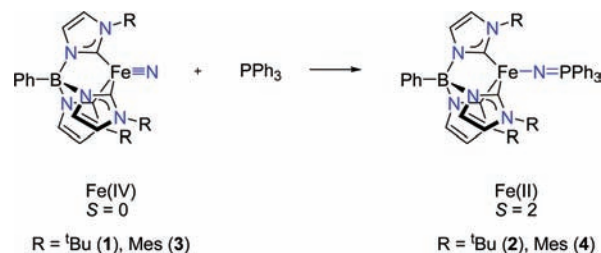


Table 1. Selected Bond Lengths for the Products of Nitrogen Atom Transfer from Iron(IV) Nitrido to PPh_3 ^a

bond length (Å)	PhB(^t BuIm) ₃	PhB(MesIm) ₃
	Fe–N=PPh ₃ (2) ²⁴	Fe–N=PPh ₃ (4) ³⁶
Fe–N	1.894(2)	1.855(2)
P=N	1.527(2)	1.524(2)
Fe–C	2.102(2)–2.151(2)	2.079(2)–2.089(2)

^aData shown for high spin ($S = 2$) states only.

in formation of the iron(II) phosphoraniminato complexes **2** and **4**, as characterized by X-ray crystallography and ^1H NMR spectroscopy (Scheme 1). Both phosphoraniminato complexes adopt a high spin ($S = 2$) state at room temperature, although **4** undergoes spin crossover to the low spin ($S = 0$) form in the solid state, with $T_C = 81$ K.^{24,36}

X-ray crystallographic characterization of these complexes revealed the complexes to have similar structures, with most of the metrical parameters around the iron atom in the two complexes comparable (Table 1). The most notable structural difference relates to the phosphoraniminato ligand. Specifically, the Fe–N bond length (1.855(2) Å) in **4** is almost 0.05 Å shorter than the corresponding bond distance in **2** (1.894(2) Å), which is likely because of the different steric demands of the two tris(carbene)borate ligands.

Similarly to our previous observations, **1** also reacts cleanly with PMe_2Ph , PMePh_2 , and $\text{P}(\text{OPh})_3$ to yield the corresponding high spin ($S = 2$) iron(II) products of nitrogen atom transfer. No reaction was observed between **1** and P^tBu_3 . Likewise, complex **3** also reacts with *para*-substituted triarylphosphines $\text{P}(p\text{-XC}_6\text{H}_4)_3$ and the phosphites $\text{P}(\text{OR})_3$ to quantitatively yield the corresponding high spin iron(II) phosphoraniminato complexes, $\text{PhB}(\text{MesIm})_3\text{Fe}-\text{N}=\text{P}(p\text{-XC}_6\text{H}_4)_3$ and $\text{PhB}(\text{MesIm})_3\text{Fe}-\text{N}=\text{P}(\text{OR})_3$ ($R = \text{Me}, \text{Ph}$).

Kinetics Experiments. As described above, our previous report revealed little difference in the rates of reaction between **1** and a series of *para*-substituted triarylphosphines.²² We have now measured the rate of nitrogen atom transfer from **1** to substrates having a broader range of steric and electronic properties, namely, PMe_2Ph , PMePh_2 and $\text{P}(\text{OPh})_3$. There is an excellent correlation between the rate of nitrogen atom transfer from **1** to this series of substrates and the size of the phosphorus nucleophile as measured by the Tolman cone angle (Figure 3), but no dependence on any electronic parameter, for example, pK_a or $\chi(\text{CO})$.²⁷ We have also examined the influence of solvent on the rate of nitrogen atom transfer, and find no significant difference in the rate for the reaction between **1** and PPh_3 in THF ($k_2 = 4.0 \pm 0.2 \times 10^{-4} \text{ M}^{-1} \text{ s}^{-1}$)²² and toluene ($k_2 = 5.67 \pm 0.06 \times 10^{-4} \text{ M}^{-1} \text{ s}^{-1}$) at 298 K.

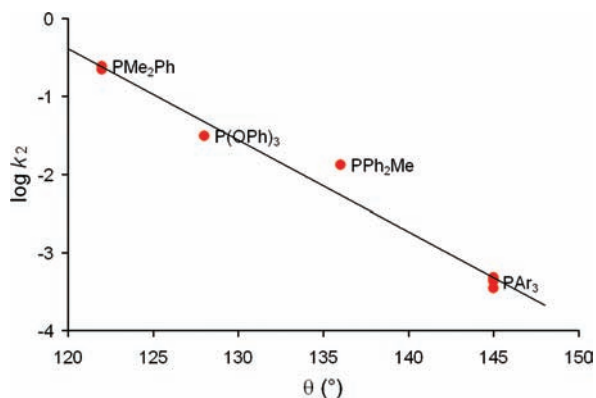


Figure 3. Plot of $\log k_2$ versus Tolman cone angle for the reaction of **1** with a series of phosphines and phosphites. Rates of reaction were measured in THF at 298 K.

An isosbestic point is observed at 435 nm when the reaction between **3** and excess PPh₃ is measured by UV–vis spectroscopy (toluene, 299 K). In contrast to **1**, nitrogen atom transfer from **3** to PPh₃ is swift, requiring the use of rapid-scan methods to measure the rates of reaction. The pseudo first-order rate constants are proportional to [PPh₃], corresponding to the rate law, $\text{rate} = k_2[3][\text{PPh}_3]$ with no evidence for saturation kinetics in the substrate concentration range used (5.2–27.5 mM). Higher phosphine concentrations resulted in rates beyond the limit of the rapid-scan instrument. The second order rate law is the same as determined for the reaction of **1** with PPh₃, but with a significantly larger second order rate constant (Table 2).

An Eyring analysis of the temperature dependent rate constants (10 °C–50 °C) gives activation parameters $\Delta H^\ddagger = 3.9 \pm 0.2$ kcal/mol and $\Delta S^\ddagger = -41 \pm 3$ e.u. (Table 2). The activation entropies are similar for both nitrido complexes and are consistent with an associative process. The dramatically enhanced rate of nitrogen atom transfer from **3** to PPh₃ is principally driven by the lower enthalpy of activation.

To acquire information about the electronic nature of the nitrogen atom transfer reaction, we also investigated the rate of nitrogen atom transfer to a series of *para*-substituted triarylphosphines. The rates of reaction between **3** and P(*p*-XC₆H₄)₃ were measured in toluene, as was done for the reaction with PPh₃. Unexpectedly, electron-withdrawing substituents were observed to *increase* the rate of reaction, as shown in a Hammett plot (Figure 4). There is excellent correlation ($r = 0.92$) with the Hammett parameter σ , and the Hammett ρ value (0.52 ± 0.10), while modest, is *opposite* in sign that expected for an electrophilic nitrido ligand.

Further insight into the electronics of the nitrogen transfer reaction from **3** was obtained from competition experiments between PPh₃ and the two phosphites P(OMe)₃ and P(OPh)₃. These experiments reveal that nitrogen atom transfer to PPh₃ is an order of magnitude faster than to either of the phosphites. A separate competition experiment involving P(OMe)₃ and P(OPh)₃ reveals that nitrogen atom transfer to P(OPh)₃ is three times faster than to P(OMe)₃.

Computational Investigations. The results of calculations are summarized in Table 3. Reactant **3** is found to have a singlet ground state at the B3LYP level of theory, with a short Fe–N bond (1.491 Å). The triplet and quintet states lie respectively 7.9 and 30.4 kcal/mol higher in energy, and have significantly

Table 2. Kinetic Parameters for the Reaction of Iron(IV) Nitridos with Triarylphosphines

	PhB(^t BuIm) ₃ Fe≡N (1) ²⁴	PhB(MesIm) ₃ Fe≡N (3)
k_2 (M ⁻¹ s ⁻¹ , 299 K) ^a	$4.0 \pm 0.2 \times 10^{-4}$	$1.44 \pm 0.02 \times 10^3$
ΔH^\ddagger (kcal/mol) ^a	13.7 ± 0.1	3.9 ± 0.2
ΔS^\ddagger (e.u.) ^a	-30 ± 1	-41 ± 3
ΔG^\ddagger (kcal/mol, 299 K) ^a	22.7 ± 0.3	16.2 ± 0.8
ρ^b	-0.04 ± 0.03	0.52 ± 0.10

^a Kinetic data for reaction with PPh₃. ^b Hammett ρ value for a series of *para*-substituted triarylphosphines.

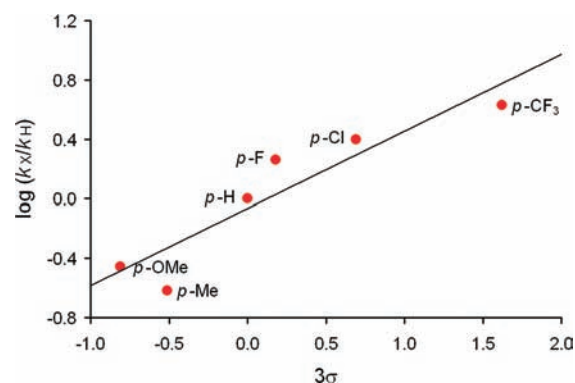


Figure 4. Hammett plot for the reaction of **3** with P(*p*-XC₆H₄)₃. Rates of reaction were measured in toluene at 299 K. The ordinate is $3\sigma_p$ to account for the trisubstitution of the phosphine.³⁷

Table 3. Relative Energies (kcal/mol) Calculated at the B3LYP Level of Theory^a

species	B3LYP	B3LYP-D3	B3LYP-D3/PCM
¹ 3	0.0	0.0	0.0
³ 3	8.3	7.4	6.2
⁵ 3	31.4	31.6	30.5
¹ 3 + PPh ₃ TS	11.7	-12.2	-0.2
¹ 4	-25.7	-58.1	-50.5
³ 4	-26.1	-53.9	-42.6
⁵ 4	-44.5	-66.7	-52.2
¹ 3 + POME ₃ TS	17.1	4.5	8.7
¹ 3 + P(<i>p</i> -C ₆ H ₄ -CF ₃) ₃ TS	5.4	-13.6	2.7

^a The B3LYP level of theory includes dispersion correction (B3LYP-D3), and the B3LYP-D3 level includes continuum solvent (B3LYP-D3/PCM). In each case, zero-point energy corrections are included.

elongated Fe–N bonds (1.552 Å and 1.614 Å respectively), with some spin density on the nitrogen atom (0.08 and 0.45 unpaired electrons, respectively). As shown in Figure 2, the HOMO of the nitride singlet ground state is a degenerate pair of orbitals that are largely nitrogen lone pairs of π symmetry with respect to the Fe–N bond. The LUMO is best described as an Fe–N σ^* orbital, with significant nitrogen character.

The singlet TS for addition of PPh₃ to **3** to form **4** lies 11.7 kcal/mol above reactants, and involves a nearly end-on approach of the phosphorus to the metal nitride group ($r_{\text{Fe-N}} = 1.530$ Å, $r_{\text{N-P}} = 2.328$ Å, angle Fe–N–P = 178.0°). The rather

small increase in the Fe–N distance compared to reactants, and the long N–P distance, reflect the very early nature of the TS, readily explained by the exothermic nature of the addition step (see below). The phosphine approaches in a collinear and largely symmetric way, with the three N–P–C(Ph) angles at 118.0, 111.2, and 107.7°. The scatter in these angles might be due to the lack of rigorous C_3 symmetry, but is more likely to be due to the orbital interactions described in more detail for the case of the CF_3 -substituted phosphine below.

The computed barrier height at the B3LYP level is somewhat larger than the observed enthalpy of activation, and this is most likely due to the poor description of dispersion interactions at the B3LYP level, as has been found previously in some other reactions in which two or more nonpolar moieties are brought together in the TS.³⁸ Using the B3LYP-D3 correction scheme of Grimme et al.³⁴ lowers the TS very significantly, so that it lies well below the reactants in energy. This large lowering arises because of the extensive number of new C–C nonbonded interactions between the P-Ph and N-mesityl rings formed at the TS. Had we been able to carry out B3LYP-D3 optimization of the TS, a slightly earlier and higher energy TS would most likely have been found, as the inclusion of dispersion effects lowers the energy at small N–P distances more than at high distances. Indeed, B3LYP geometry optimization holding the N–P distance frozen at 2.5 and 2.7 Å, followed by B3LYP-D3 correction, leads to a local maximum of the B3LYP-D3 energy near $r = 2.5$ Å, about 1 kcal/mol above the B3LYP-D3 energy at the B3LYP TS structure. Computing the B3LYP-D3 energy of the TS in vacuum neglects the contribution to the barrier height from the significant loss of dispersion energy incurred by desolvation of the parts of the phosphine and reactant surface that come into close contact in the TS and the product. This effect is partially accounted for by the continuum solvent model, which raises the barrier by 12.0 kcal/mol, leading to a B3LYP-D3+continuum barrier height of –0.2 kcal/mol, somewhat below, but in acceptable agreement with, the experimental activation enthalpy of 3.9 kcal/mol. This level of agreement is certainly within the expected uncertainties in the B3LYP method and the B3LYP-D3 correction.

The product 4 is computed to have a quintet ground state at the B3LYP level of theory, in agreement with experiment, and the quintet lies well below reactants at the B3LYP level of theory, with the very exothermic addition accounting for the very early addition TS. The triplet and singlet states also lie well below the energy of reactants, but lie much higher in energy than the quintet state at the B3LYP level. All these species have typical strong N–P double bond character, with computed bond lengths rN–P of 1.541 Å, 1.553 Å, and 1.572 Å respectively. The former value is in reasonable agreement with the experimental result of 1.524 Å for the quintet product. The adducts have significantly extended Fe–N distances compared to the reactant, for example, 1.868 Å and 1.820 Å for the quintet and singlet, respectively, with the former again agreeing well with experiment (1.855 Å). Experimentally, the quintet product is found to undergo crossover to the singlet, and this is not consistent with the much higher energy computed for the latter at the B3LYP level. The discrepancy can again be understood considering the poor description of dispersion by B3LYP, an effect which is more important in product than reactants, and is especially important in the more compact singlet. The B3LYP-D3 correction lowers the energy of the singlet by a large amount (31.5 kcal/mol) compared to reactants, and although the quintet is also stabilized (by 12.8 kcal/mol), the net effect is to bring the

singlet and quintet close in energy. Including the continuum solvent correction, the product singlet and quintet states are predicted to lie very close in energy, in good agreement with the fact that they undergo spin crossover. The triplet lies significantly higher in energy at this level of theory.

On the basis of the calculations, addition of phosphine is predicted to lead to singlet product **4** initially. On the basis of previous experience,³⁹ the singlet and quintet surfaces should cross at low relative energies, so that spin crossover to form the quintet is likely to proceed rapidly, with a unimolecular rate constant of 10^6 s^{–1} or greater, such that the kinetically observed product will be the quintet.

The TSs for addition of trimethylphosphite and tris(*para*-trifluoromethylphenyl)phosphine to the nitride 3 have structures and relative energies that are qualitatively similar to those found for triphenylphosphine. In more detail, though, the differences in relative energy and in structure are of significant interest in understanding the experimental data. The phosphite addition TS lies significantly higher in relative energy than the phosphine TS, in agreement with the observed lower reactivity, at all levels of theory shown in Table 3. This is not unexpected given the well-known lower σ -donor character of phosphites compared to phosphines. Note that the conformational complexity in this system is considerable, as trialkylphosphites exist in several close-lying conformeric minima.⁴⁰ Here, we have considered the conformer with a (*gauche-gauche-anti*) arrangement of the three methyl groups with respect to the P lone pair, in both the free phosphine and the TS. This TS has a rather linear approach of the phosphorus to the Fe–N group (Fe–N–P angle of 175.1°), as for the phosphite, but is significantly distorted from C_3 symmetry when considering the three N–P–O angles at the TS (101.2°, 101.6°, and 150.8°). The methoxy group with the large N–P–O angle is one of the two with a *gauche* arrangement, which have a higher effective steric requirement, and hence this low symmetry could reflect the steric effects.

It is also possible that nonbonded interactions between 3 and the phosphine play a role in the substituent effect. The very large impact of the dispersion energy correction on the TS energies highlights the important role of nonbonded interactions on reactivity in these systems. While the dispersion component of the energy should not in itself lead to a large substituent effect, it is possible that other nonbonded interactions between the phosphine aryl groups and the mesityl rings of 3 play a role. As the mesityl rings will be quite electron-rich, they may have a more attractive interaction with the more electron-poor P(*p*-C₆H₄CF₃)₃ than with PPh₃. This may be an additional effect contributing to the observed reactivity pattern.

However, the trifluoromethyl-substituted TS has an energy and a structure such that another effect must be considered to play an important role in reactivity, and this presumably also intervenes for the other cases also. The TS is found to lie lower in energy than that for PPh₃, at just 5.4 kcal/mol relative to reactants at the B3LYP level of theory. This agrees in qualitative terms with the calculated higher reactivity of the trifluoromethylphenyl phosphine with the iron nitride compared to triphenylphosphine. The latter experimental observation is surprising, so it is pleasing that the same trend is observed computationally (albeit not upon including the continuum solvent correction, though considering the likely error bars this is not inconsistent with the experimental trend). The calculations also provide insight into this effect. The trifluoromethyl-substituted TS is found to be even earlier than the parent TS, with rFe–N = 1.495 Å, and

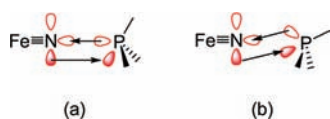


Figure 5. Orbital interactions in the transition state for nitrogen atom transfer, showing that the interactions are symmetry-allowed in both the linear (a) and the bent (b) structures. In (a), the σ donation from the P lone pair to the nitride LUMO is favored. In (b), σ donation is relatively less important compared to π donation from the N lone pair to the P-X σ^* orbitals.

rN-P = 2.765. More importantly, it is found to have the same distortion as the parent TS and the phosphite TS, with a fairly linear Fe-N-P angle of 175.9° but three rather different N-P-C angles, of 103.6° , 104.1° , and 129.0° .

This distortion can be attributed to a key orbital interaction at the TS, whereby, as well as electron donation from the P lone pair to the Fe-N σ^* orbital, donation from the N lone pairs of π symmetry into the low-lying P-C σ^* orbitals of the phosphine is also important (Figure 5). Note that while the HOMO and HOMO-1 of **3** have only partial N lone pair character, there are several other high-lying occupied orbitals with N lone pair character, and upon approach by the phosphine, these orbitals can mix to provide greater N lone pair character to the HOMO. Both the P \rightarrow LUMO and N \rightarrow P-C σ^* interactions are symmetry-allowed even with a completely symmetric approach of the phosphine. The bending distortion will tend to decrease the strength of the P lone pair donation to the nitride LUMO, but the interactions between the two N lone pairs and the π -symmetry-adapted combinations of P-X σ^* orbitals will be maintained. The occurrence of this orbital effect is supported by the Mulliken charges. In free PPh₃ and P(*p*-C₆H₄CF₃)₃, the phenyl and aryl groups have partial charges of -0.115 and -0.126 , respectively, with the phosphorus having a compensating positive charge of 0.345 and 0.378 . In the PPh₃ TS, the phosphine overall acquires a positive charge of $+0.132$ and the aryl groups also become less negative. In the trifluoromethylphenyl case, the phosphine overall becomes negative (albeit only at -0.025) and the aryl ring with the largest N-P-C angle becomes more negative, at -0.130 . Orbital plots of the HOMO of **3** and the HOMO-1 of the addition TS (Supporting Information, Figure S8), also support the occurrence of this orbital interaction. One might expect that this interaction would lengthen the P-C bonds at the TS, but considering these bond lengths (Supporting Information, Table S8), it can be seen that they shorten from the reactant to the TS, probably because of changes in hybridization at phosphorus, and any change due to N lone pair donation into the σ^* orbitals cannot be detected.

It is interesting to note, finally, that in the model system used to compute zero-point energies, with the small PH₃ nucleophile, and no substituents on the carbene ligands, the TS (rN-P = 1.959 \AA) is even more distorted, with an Fe-N-P angle of 162.6° , and N-P-H angles of 99.3° (twice) and 160.3° . This may reflect a slightly different electronic character of the TS, but may also be the preferred TS structure in the absence of steric effects, that favor a more symmetric structure in the "real" system.

DISCUSSION

As with our previous report on nitrogen atom transfer from **1** to PPh₃, the rate law for the corresponding reaction of **3** is consistent with an associative mechanism involving phosphine

attack at the nitrido ligand. An outer sphere mechanism that involves initial electron transfer prior to N-P bond formation can be excluded on two counts: (1) neither iron nitrido complex can be reduced at potentials above -2.5 V (vs. Cp₂Fe⁺/Cp₂Fe)^{24,41} and therefore triphenylphosphine ($E_{\text{ox}} \approx 0.6 \text{ V}$ vs Cp₂Fe⁺/Cp₂Fe)⁴² is thermodynamically incapable of reducing the nitrido complexes to iron(III), and (2) the solvent polarity has no effect on the rate of reaction between **1** and PPh₃, which is inconsistent with the formation of charged intermediates. Thus, these data are most consistent with an inner sphere reaction involving nitrogen atom transfer from [Fe≡N] unit to the phosphine.

Steric Effects on Nitrogen Atom Transfer. As previously mentioned, in our previous report no electronic effect was observed in the rate of nitrogen atom transfer from **1** to triarylphosphines. We tentatively ascribed this result to steric effects, where interactions involving the bulky *tert*-butyl substituents of the tris(carbene)borate ligand result in a congested transition state that overwhelms any electronic factors. Extending the substrate scope to include a range of sterically differentiated phosphines as well as an electronically dissimilar phosphite provides more compelling evidence for this conclusion. Specifically, there is an excellent correlation between the rate of reaction and the size of the phosphine, as measured by the Tolman cone angle (Figure 3), with more than a 2 orders of magnitude difference in rate between the smallest and the largest phosphine. Furthermore, there is no correlation between the rate of reaction and any electronic parameter for the phosphorus(III) substrate.²⁷

Complex **3** also undergoes two-electron nitrogen atom transfer to phosphines; however the reaction rate is dramatically faster, with the second order rate constant for the reaction with PPh₃ 7 orders of magnitude larger than for **1** (Table 2). While there is a small difference in the donor strength of the two tris(carbene)borate ligands,⁴³ the HOMOs and LUMOs of the iron nitridos are largely nonbonding with respect to these ligands,^{22,44} which is expected to mitigate any electronic differences. The more rapid reaction rate for **3** is largely related to the smaller ΔH^\ddagger , that is, the formation of a P=N double bond at the expense of two Fe=N π bonds. Thus, formation of the transition state requires less bond breaking in the case of **3** than for **1**, and is likely a consequence of the different topologies of the two tris(carbene)borate ligands. Specifically, the planar mesityl substituents in **3** allow the incoming substrate to be closer to the iron center, which reduces the extent of Fe-N bond breaking required to reach the transition state. Consistent with this idea, the only significant difference between the solid state structures of the products ($S = 2$ spin state) are the Fe-N bond lengths, with the Fe-N bond in **4** being shorter. Thus, for iron(IV) nitrido complex **1**, the bulkiness of the tris(carbene)borate ligand overwhelms any electronic factors.

Electronic Effects. The reduced impact of steric effects for complex **3** has allowed us to probe the effect of electronic factors on the rate of nitrogen atom transfer. The rate constants for nitrogen atom transfer to a series of *para*-substituted triarylphosphines correlate well with the Hammett parameter σ , but the observed positive ρ value is unexpectedly *opposite* in sign to that expected for an electrophilic nitrido ligand. While we are unaware of any Hammett studies for nitrogen atom transfer to phosphines, the rate of two electron nitrogen atom transfer from TpOs(N)X₂ (X = Cl, Br, OAc, O₂CCF₃, O₂CCl₃, O₂CCBr₃, ONO₂, X₂ = O₂C₂O₂) to PPh₃ follows the trend expected for an electrophilic nitrido ligand (i.e., electron poor nitrido complexes react faster), although the effect is modest.²¹

The analogous two-electron oxygen atom transfer reaction has been more extensively studied, and to the best of our knowledge, all Hammett studies are consistent with nucleophilic attack of the phosphine at an electrophilic oxo group. Thus, Hammett studies on oxygen atom transfer to triarylphosphines typically give a negative ρ value (e.g., for $\text{MeReO}(\text{mtp})\text{PPh}_3$ ($\text{mtp} = 2$ -(mercaptomethyl)thiophenol), $\rho = -0.70$);⁴⁵ for $(\text{Mes})_3\text{Ir}=\text{O}$, $\rho = -0.29$ ⁴⁶), as expected for an electrophilic oxo ligand. Therefore, the positive ρ value for nitrogen atom transfer from **3** to triarylphosphines appears to be without precedent.

We further investigated this apparent nucleophilicity by determining the relative rate of nitrogen atom transfer to the phosphites $\text{P}(\text{OMe})_3$ and $\text{P}(\text{OPh})_3$. Intriguingly, these phosphites react an order of magnitude more slowly than PPh_3 , and with little dependence on their size. These rate differences can be ascribed to the lower relative σ -basicity of the phosphites, and are most consistent with an electrophilic nitrido ligand.

Given these seemingly contradictory results, we turned to density functional theory calculations to obtain insight into the electronic characteristics of the nitrogen atom transfer reaction. Since nitrogen atom transfer from **3** to phosphines is spin forbidden, we first investigated the influence of spin state changes on the reaction energetics. Spin state changes have previously been shown to have an impact on the mechanism of oxygen atom transfer from d^0 and d^1 metal oxo complexes.^{9,47}

The relative energies for all likely spin states for the reactants and products have been calculated for the full system and also for a model system in which a simplified tris(carbene)borate ligand and phosphine have been used. The results of these calculations are self-consistent, and therefore only the results of the full system will be discussed here. The calculations show that the spin state change from reactants to products is unlikely to have any influence on the rate of nitrogen atom transfer. Specifically, we find that for the phosphoraninato product **4**, the singlet state ($S = 0$) is lower in energy than the singlet state for the nitrido and phosphine reactants (**3** + PPh_3) (Figure 6). Furthermore, because of the large energy difference between the $S = 0$ and $S = 2$ states of **3**, a change in spin state prior to N–P bond formation is unlikely to be kinetically accessible. Thus, these computational results are most consistent with nitrogen atom transfer occurring on the singlet surface to give a singlet product, followed by a rapid spin state change to the quintet product. In support of this idea, we note that **4** undergoes a thermal spin crossover at low temperature, as expected for energetically accessible $S = 0$ and $S = 2$ spin states. This spin crossover occurs at 81 K in the solid state.³⁶ Attempts to probe this spin state change in solution by VT-NMR showed no evidence for a spin state change at temperatures down to 198 K, and the $S = 2$ state is thermodynamically favored in solution at room temperature. Although we do not know the rate of spin crossover for **4**, in cases where the kinetics of spin crossover in solution has been investigated, the rate constant is typically $>10^5 \text{ s}^{-1}$.⁴⁸ In sum, the computational and experimental data suggest that the $S = 0$ to $S = 2$ spin transition is not rate determining for the reaction of **3** with PPh_3 .

To obtain insight into the unusual electronic character of the reaction we calculated the transition state on the singlet surface. The B3LYP calculations provide good qualitative insight, though neglect of dispersion interactions and solvation effects leads to less good quantitative agreement with experiment. An attempt to treat these two effects has therefore also been included, using the –D3 dispersion correction³⁵ and a polarizable continuum

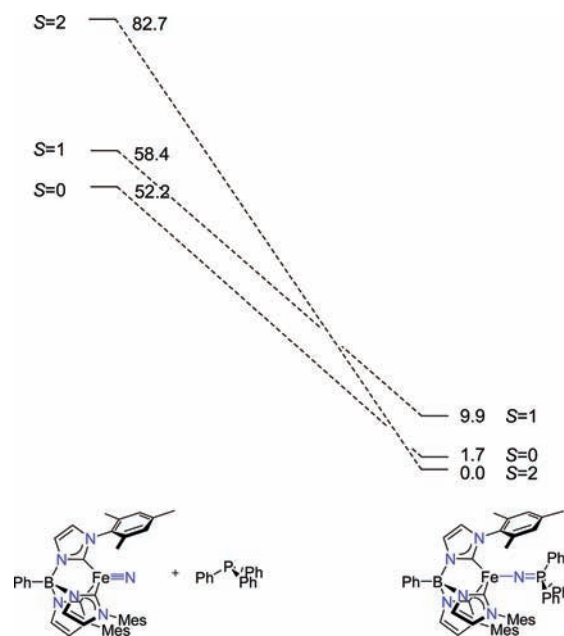


Figure 6. Relative energies of all possible spin states for the reaction $\text{PhB}(\text{MesIm})_3\text{Fe}\equiv\text{N} + \text{PPh}_3 \rightarrow \text{PhB}(\text{MesIm})_3\text{Fe}=\text{N}=\text{PPh}_3$, including dispersion corrections and solvent effects (B3LYP-D3/PCM). Energies are in kcal/mol, and are relative to that of $\text{PhB}(\text{MesIm})_3\text{Fe}=\text{N}=\text{PPh}_3$ ($S = 2$). See Table 3 and the text for further details on the computational methods.

model (PCM), as discussed in the results section. For the full system, the transition state is calculated to lie 0.2 kcal/mol below the reactants' ground state energy at the B3LYP-D3+PCM level of theory, consistent with the rapid reaction rate that is observed experimentally, and providing further evidence that P–N bond formation occurs on the singlet surface. Similar results are obtained for calculations on a model system. Interestingly, the calculated transition state structure shows that the phosphorus atom adopts a sawhorse geometry (Figure 7), instead of the intuitively anticipated trigonal pyramidal geometry. This geometric preference is indicative of a dual-nature interaction involving a σ -symmetry interaction between the nitrido LUMO (nitrido a_1 orbital) and phosphine HOMO (phosphorus lone pair) in addition to a π -symmetry interaction between the nitrido HOMO (nitrido $e_{(a)}$ orbital) and phosphine LUMO ($\text{P}-\text{C} \sigma^*$ orbital) (Figure 5). Charge analysis of the electronic wave function at the TS supports this interpretation: though the phosphine moiety develops a positive charge in the case of PPh_3 addition, it acquires a small negative charge in the case of addition of $\text{P}(p\text{-C}_6\text{H}_4\text{CF}_3)_3$. The calculated transition state thereby provides a rationale for the results of the Hammett study because the π -symmetry interaction leads to the transfer of electron density from the nitrido ligand to the phosphine. Thus, the nitrido ligand also has nucleophilic character.

This finding also explains why nitrogen atom transfer from **3** to the bulkier, more π -acidic phosphite $\text{P}(\text{OPh})_3$ is faster than $\text{P}(\text{OMe})_3$. Moreover, our recent report of nitrogen atom transfer from the iron(IV) nitrido complexes to CO and CN^tBu provides experimental evidence that the nitrido ligands have nucleophilic character.⁴⁹ In particular, the facile reaction with the weak σ -base CO is consistent with the hypothesis that nitrogen atom transfer also involves an interaction between the iron nitrido $e_{(a)}$ and the substrate π^* orbitals.

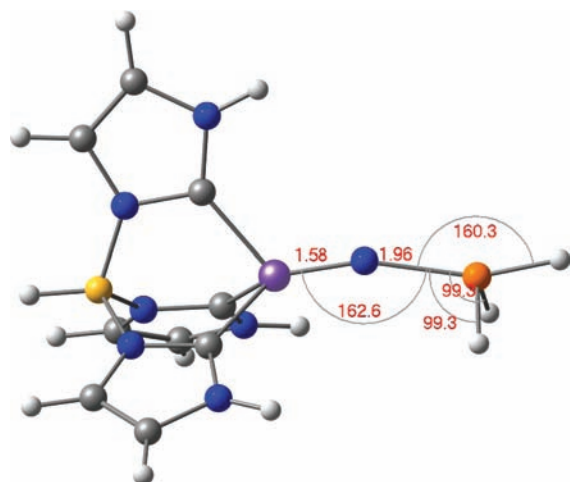


Figure 7. Calculated transition state for nitrogen atom transfer in the model system $\text{HB}(\text{MeIm})_3\text{Fe}\equiv\text{N} + \text{PH}_3$. Selected bond lengths (Å) and angles (deg) are shown.

Although we are unaware of a similar Hammett studies for oxygen atom transfer from metal oxo complexes to phosphines, there have been some suggestions that the transition state for oxygen atom transfer to phosphorus(III) substrates has partial nucleophilic character. For example, the rate of oxygen atom transfer from $\text{MeRe}(\text{NAr})_2\text{O}$ ($\text{Ar} = 2,6$ -diisopropylphenyl) was found to be greater for π -acidic $\text{P}(\text{OR})_n\text{R}'_{3-n}$ substrates than for phosphines.^{50,51} Furthermore, although direct experimental evidence is lacking, the transition state for oxygen atom transfer from $\text{Tp}^{\text{iPr}_2}\text{MoO}_2(\text{OPh})$ to phosphines, calculated by electronic structure theory, has been proposed to involve oxo nucleophilic attack on the $\text{P}-\text{C}$ σ^* orbital in addition to the expected nucleophilic attack of the phosphorus lone pair on the $\text{Mo}=\text{O}$ π^* orbital.⁵²

Implications for Atom and Group Transfer in 3-Fold Symmetry. While it is well-known that metal–ligand multiple bonds in late transition metal complexes can be stabilized in 3-fold symmetry,⁵³ the factors that influence their reactivity in group transfer reactions are still poorly understood. Furthermore, although the mechanism of nitrogen atom transfer to phosphines has generally been considered to involve nucleophilic attack of the phosphine at a vacant orbital at the nitrido ligand,²¹ our results show that more subtle interactions are involved in these reactions.

It is instructive to compare two electron nitrogen atom transfer from **3** with the equivalent oxygen atom transfer from $(\text{Mes})_3\text{Ir}=\text{O}$.⁵⁴ The pseudotetrahedral iridium complex, whose atom transfer reactivity has been studied in some detail,^{8,44} is isoelectronic (d^4 , $S = 0$) with **3** and has an analogous electronic structure. However, when compared to **3**, the rate of phosphine oxidation is orders of magnitude slower for $(\text{Mes})_3\text{Ir}=\text{O}$, and the electronic selectivity of $(\text{Mes})_3\text{Ir}=\text{O}$, although modest, is *opposite* to that of **3**.

In the case of $(\text{Mes})_3\text{Ir}=\text{O}$, although oxygenation of PPh_3 is relatively slow ($k = 3.95(5) \text{ M}^{-1} \text{ s}^{-1}$, 293 K),⁴⁴ oxygen atom self-exchange is ultrafast ($k_{\text{Ir}} = 5 \times 10^7 \text{ M}^{-1} \text{ s}^{-1}$ from low temperature data extrapolated to 293 K),⁸ which suggests that the slow rate of the former reaction is kinetic, and not thermodynamic, in origin. Indeed, the slow rate of phosphine oxidation is attributed in part to strong destabilization of the pseudotetrahedral geometry in the successor $(\text{Mes})_3\text{Ir}(\text{OPPh}_3)$ complex. This

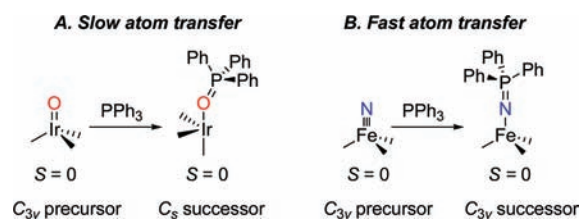


Figure 8. Geometric preferences of atom transfer reactions in 3-fold symmetry.

successor complex strongly favors a *cis*-divacant octahedron (sawhorse) geometry, as expected for a four-coordinate d^6 $S = 0$ complex (Figure 8A).⁵⁵ This geometric mismatch introduces a kinetic barrier that is believed to prevent oxygen atom transfer to substrates such as Me_2SO and allyl alcohol, despite these reactions being thermodynamically favorable.

By contrast, the combination of a small bite angle tridentate ligand (i.e., a tris(carbene)borate) and strong π -donor axial ligand³² stabilizes the $S = 0$ (d^6) state for the pseudotetrahedral geometry of $\text{PhB}(\text{MesIm})_3\text{Fe}-\text{N}=\text{PPh}_3$, the initial product of atom transfer (Figure 8B). Similar stabilization of low spin states in other pseudotetrahedral iron(II) complexes has been reported.^{52,56} In this geometry, spin crossover to the observed $S = 2$ (d^6) phosphoraniminato product **4** is a low energy process that does not involve major structural reorganization.⁵² Thus, the combination of a 3d metal, which has a greater density of states than a 5d metal, and the rigid tris(carbene)borate supporting ligand provide access to the appropriate electronic states and geometries that allow for rapid atom transfer.

The polarity of the atom transfer reaction is another important difference between these two complexes. For $(\text{Mes})_3\text{Ir}=\text{O}$, a Hammett study with *para*-substituted triarylphosphines gave results expected for an electrophilic oxo ligand, although the effect is modest ($\rho = -0.29(10)$). This electronic difference is likely related to the relative frontier orbital energies of the iridium and iron complexes, specifically the HOMO, which determines the relative nucleophilic character of the transition state. Since symmetry considerations dictate that the $e_{(a)}$ HOMO is non-bonding in character, the relative energy of these orbitals will largely be determined by the atomic orbital energies of the metal. The HOMO of $(\text{Mes})_3\text{Ir}=\text{O}$ is therefore expected to be at lower energy than that of **2**, reducing the nucleophilic character of the oxo ligand. We note that there may be some partial nucleophilic character in the transition state for oxygen atom transfer from $(\text{Mes})_3\text{Ir}=\text{O}$ that reduces the electrophilicity of the oxo ligand, as reflected in the modest Hammett parameter, ρ .

CONCLUSIONS

The 3-fold symmetric iron(IV) nitrido complex **3** undergoes swift nitrogen atom transfer to triarylphosphines. Changing the steric profile of the supporting tris(carbene)borate from the sterically congested *tert*-butyl substituted ligand in **1** to the less constricting mesityl substituted ligand in **3** facilitates atom transfer by removing inhibiting steric interactions, revealing the rapid intrinsic rate of nitrogen atom transfer from these complexes. The rapid rate of reaction is facilitated by a dual nature transition state that involves both HOMO and LUMO of the iron complex. It is likely that the π symmetry interaction involving the iron nitrido HOMO (akin to π backbonding in transition metal

complexes) will facilitate nitrogen atom transfer to other substrates that can accept π electron density, for example, alkenes.

More generally, it has previously been shown that rate of atom transfer can be increased by making the complex more electrophilic, for example, by increasing the charge on the complex.⁵⁷ Our results suggest a complementary strategy for increasing the rate of atom transfer: increasing the nucleophilicity of the atom to facilitate the dual nature transition state. This strategy is likely to be most applicable for 3d transition metal complexes, where HOMO is relatively high in energy and the density of states is large. A caveat to this strategy, as exemplified by the slower reaction with phosphites, is that the relative importance of these properties may be different for different substrates. An important observation from our studies is that the electronic plasticity of first row transition metals can be harnessed to effect faster atom transfer reactivity than related complexes of the heavier elements.

ASSOCIATED CONTENT

S Supporting Information. Further kinetic additional computational results. This material is available free of charge via the Internet at <http://pubs.acs.org>.

AUTHOR INFORMATION

Corresponding Author

*E-mail: jeremy.harvey@bristol.ac.uk (J.N.H.), jesmith@nmsu.edu (J.M.S.).

ACKNOWLEDGMENT

J.M.S. acknowledges funding from the DOE-BES (DE-FG02-08ER15996) and the Dreyfus Foundation. We thank Michael D. Johnson (NMSU) for providing access to his OLIS rapid scan instrument.

REFERENCES

- (1) Abu-Omar, M. M. In *Physical Inorganic Chemistry*; Bakac, A., Ed.; Wiley: Hoboken, NJ, 2010; Chapter 3.
- (2) (a) Sono, M.; Roach, M. P.; Coulter, E. D.; Dawson, J. H. *Chem. Rev.* **1996**, *96*, 2841–2887. (b) Denisov, I. G.; Makris, T. M.; Sligar, S. G.; Schlichting, I. *Chem. Rev.* **2005**, *105*, 2253–2277.
- (3) Coates, J. D.; Achenbach, L. A. *Nat. Rev. Microbiol.* **2004**, *2*, 569–580.
- (4) Costas, M.; Mehn, M. P.; Jensen, M. P.; Que, L., Jr. *Chem. Rev.* **2004**, *104*, 939–986.
- (5) Abu-Omar, M. M.; Loaiza, A.; Hontzeas, N. *Chem. Rev.* **2005**, *105*, 2227–2252.
- (6) (a) Hille, R. *Chem. Rev.* **1996**, *96*, 2757–2816. (b) Hille, R. *Trends Biochem. Sci.* **2002**, *27*, 360–367.
- (7) (a) Holm, R. H. *Chem. Rev.* **1987**, *87*, 1401–1449. (b) Holm, R. H.; Donahue, J. P. *Polyhedron* **1993**, *12*, 571–589.
- (8) Fortner, K. C.; Laitar, D. S.; Muldoon, J.; Pu, L.; Braun-Sand, S. B.; Wiest, O.; Brown, S. N. *J. Am. Chem. Soc.* **2007**, *129*, 588–600.
- (9) (a) Veige, A. S.; Slaughter, L. M.; Wolczanski, P. T.; Matsunaga, N.; Decker, S. A.; Cundari, T. R. *J. Am. Chem. Soc.* **2001**, *123*, 6419–6420. (b) Veige, A. S.; Slaughter, L. M.; Lobkovsky, E. B.; Wolczanski, P. T.; Matsunaga, N.; Decker, S. A.; Cundari, T. R. *Inorg. Chem.* **2003**, *42*, 6204–6224.
- (10) (a) Figueroa, J. S.; Piro, N. A.; Clough, C. R.; Cummins, C. C. *J. Am. Chem. Soc.* **2006**, *128*, 940–950. (b) Curley, J. J.; Sceats, E. L.; Cummins, C. C. *J. Am. Chem. Soc.* **2006**, *128*, 14036–14037.
- (11) Woo, L. K. *Chem. Rev.* **1993**, *93*, 1125–1136.
- (12) Selected recent examples: (a) Huynh, M. H. V.; Jameson, D. L.; Meyer, T. J. *Inorg. Chem.* **2001**, *41*, 5062–5063. (b) Bennett, B. K.; Saganic, E.; Lovell, S.; Kaminsky, W.; Samuel, A.; Mayer, J. M. *Inorg. Chem.* **2003**, *42*, 4127–4134. (c) Fang, G.-S.; Huang, J. S.; Zhu, N.; Che, C.-C. *Eur. J. Inorg. Chem.* **2004**, 1341–1348. (d) Yi, X.-Y.; Lam, T. C. H.; Sau, Y.-K.; Zhang, Q.-F.; Williams, I. D.; Leung, W.-H. *Inorg. Chem.* **2007**, *46*, 7193–7198. (e) Besson, B.; Geletii, Y. V.; Villain, F.; Villanneau, R.; Hill, C. L.; Proust, A. *Inorg. Chem.* **2009**, *48*, 9436–9443.
- (13) (a) Kwong, H.-K.; Man, W.-L.; Xiang, J.; Wong, W.-T.; Lau, T.-C. *Inorg. Chem.* **2009**, *48*, 3080–3086. (b) Tran, B. L.; Pink, M.; Gao, X.; Park, H.; Mindiola, D. J. *J. Am. Chem. Soc.* **2010**, *132*, 1458–1459.
- (14) Leung, C.-F.; Wong, T.-W.; Lau, T.-C.; Wong, W.-T. *Eur. J. Inorg. Chem.* **2005**, 773–778.
- (15) Man, W.-L.; Lam, W. W. Y.; Yiu, S.-M.; Lau, T.-C.; Peng, S.-M. *J. Am. Chem. Soc.* **2004**, *126*, 15336–15337.
- (16) Maestri, A. G.; Cherry, K. S.; Toboni, J. J.; Brown, S. N. *J. Am. Chem. Soc.* **2001**, *123*, 7459–7460.
- (17) (a) Woo, L. K.; Goll, J. G. *J. Am. Chem. Soc.* **1989**, *111*, 3755–3757. (b) Woo, L. K.; Goll, J. G.; Czaplá, D. J.; Hays, J. A. *J. Am. Chem. Soc.* **1991**, *113*, 8478–8484. (c) Neely, F. L.; Bottomley, L. A. *Inorg. Chem.* **1997**, *36*, 5432–5434. (d) Bottomley, L. A.; Neely, F. L. *Inorg. Chem.* **1997**, *36*, 5435–5439.
- (18) Chang, C. J.; Low, D. W.; Gray, H. B. *Inorg. Chem.* **1997**, *36*, 270–271.
- (19) Galubkov, G.; Gross, Z. *J. Am. Chem. Soc.* **2005**, *127*, 3258–3289.
- (20) (a) Bendix, J. *J. Am. Chem. Soc.* **2003**, *125*, 13348–13349. (b) Birk, T.; Bendix, J. *Inorg. Chem.* **2003**, *42*, 7608–7615.
- (21) Dehestani, A.; Kaminsky, W.; Mayer, J. M. *Inorg. Chem.* **2003**, *42*, 605–611.
- (22) Dehnicke, K.; Strähle, J. *Polyhedron* **1990**, *8*, 707–726, and references cited therein.
- (23) (a) Griffith, W. P.; Pawson, D. *J. Chem. Soc., Chem. Commun.* **1973**, 418–419. Pawson, D.; Griffith, W. P. *Inorg. Nucl. Chem. Lett.* **1974**, *10*, 253–255.
- (24) Scepaniak, J. J.; Fulton, M. D.; Bontchev, R. P.; Duesler, E. N.; Kirk, M. L.; Smith, J. M. *J. Am. Chem. Soc.* **2008**, *130*, 10515–10517.
- (25) The spectroscopically characterized iron(IV) nitrido complex $\text{BP}^{\text{Pr}}_3\text{Fe}\equiv\text{N}$ is reported to undergo a similar reaction with PPh_3 ; Betley, T. A.; Peters, J. C. *J. Am. Chem. Soc.* **2004**, *126*, 6252–6254.
- (26) Scepaniak, J. J.; Young, J. A.; Bontchev, R. P.; Smith, J. M. *Angew. Chem., Int. Ed.* **2009**, *48*, 3158–3160.
- (27) (a) Watt, G. W.; Baye, L. J.; Drummond, F. O., Jr. *J. Am. Chem. Soc.* **1966**, *88*, 1138–1140. (b) Brintzinger, H. H.; Bercaw, J. E. *J. Am. Chem. Soc.* **1970**, *92*, 6182.
- (28) Baker, M. V.; Field, L. D.; Hambley, T. W. *Inorg. Chem.* **1988**, *27*, 2872–2876.
- (29) See Supporting Information for full details.
- (30) Matheson, I. B. C. *Anal. Instrum.* **1987**, *16*, 345–373.
- (31) (a) Weber, B.; Walker, F. A. *Inorg. Chem.* **2007**, *46*, 6794–6803. (b) Weber, B.; Obel, J.; Henner-Vásquez, D.; Bauer, W. *Eur. J. Inorg. Chem.* **2009**, 5527–5534.
- (32) Shokhirev, N. V.; Walker, F. A. *TDF, Temperature-Dependent Fitting program*; <http://www.shokhirev.com/nikolai/programs/prgscie-du.html>.
- (33) *Jaguar*, version 7.6; Schrodinger, LLC: New York, NY, 2009.
- (34) Frisch, M. J.; Trucks, G. W.; Schlegel, H. B.; Scuseria, G. E.; Robb, M.; Cheeseman, J. R.; Montgomery, J. A.; Vreven, J. A.; Kudin, K. N.; Burant, J. C.; Millam, J. M.; Iyengar, S. S.; Tomasi, J.; Barone, V.; Mennucci, B.; Cossi, M.; Scalmani, G.; Rega, N.; Petersson, G. A.; Nakatsuji, H.; Hada, M.; Ehara, M.; Toyota, K.; Fukuda, R.; Hasegawa, J.; Ishida, M.; Nakajima, T.; Honda, Y.; Kitao, O.; Nakai, H.; Klene, M.; Li, X.; Knox, J. E.; Hratchian, H. P.; Cross, J. B.; Adamo, C.; Jaramillo, J.; Gomperts, R.; Stratmann, R. E.; Yazyev, O.; Austin, A. J.; Cammi, R.; Pomelli, C.; Ochterski, J. W.; Ayala, P. Y.; Morokuma, K.; Voth, G. A.; Salvador, P.; Dannenberg, J. J.; Zakrzewski, V. G.; Dapprich, S.; Daniels, A. D.; Strain, M. C.; Farkas, O.; Malick, D. K.; Rabuck, A. D.; Raghavachari, K.; Foresman, J. B.; Ortiz, J. V.; Cui, Q.; Baboul, A. G.; Clifford, S.; Cioslowski, J.; Stefanov, B. B.; Liu, G.; Liashenko, A.; Piskorz, P.

Komaromi, I.; Martin, R. L.; Fox, D. J.; Keith, T.; Al-Laham, M. A.; Peng, C. Y.; Nanayakkara, A.; Challacombe, M.; Gill, P. M. W.; Johnson, B.; Chen, W.; Wong, M. W.; Gonzalez, C.; Pople, J. A. *Gaussian 03*; Gaussian, Inc.: Wallingford, CT.

(35) Grimme, S.; Antony, J.; Ehrlich, S.; Krieg, H. *J. Chem. Phys.* **2010**, *132*, 154104.

(36) Scepaniak, J. J.; Harris, T. D.; Vogel, C. S.; Sutter, J.; Meyer, K.; Smith, J. M. *J. Am. Chem. Soc.* **2011**, *133*, 3824–3827.

(37) σ_p values taken from: Hansch, C.; Leo, A.; Taft, R. W. *Chem. Rev.* **1991**, *91*, 165–195.

(38) See, for example, McMullin, C. L.; Jover, J.; Harvey, J. N.; Fey, N. *Dalton Trans.* **2010**, *39*, 10833–10836.

(39) Besora, M.; Carreón-Macedo, J.-L.; Cimas, Á.; Harvey, J. N. *Adv. Inorg. Chem.* **2009**, *61*, 573–623.

(40) Ellis, D. D.; Haddow, M. F.; Orpen, A. G.; Watson, P. J. *Dalton Trans.* **2009**, 10436–10445.

(41) Scepaniak, J. J.; Vogel, C. S.; Khusniyarov, M. M.; Heinemann, F. W.; Meyer, K.; Smith, J. M. *Science* **2011**, *331*, 1049–1052.

(42) $E_{ox} \approx 1$ V vs SCE in MeCN, see: Schiavon, G.; Zecchin, S.; Cogoni, G.; Bontempelli, G. *J. Electroanal. Chem.* **1973**, *48*, 425–431. For conversion to the Cp_2Fe^+/Cp_2Fe reference, see: Connelly, N. G.; Geiger, W. E. *Chem. Rev.* **1996**, *96*, 877–910.

(43) Nieto, I.; Bontchev, R. P.; Ozarowski, A.; Smirnov, D.; Krzystek, J.; Telsler, J.; Smith, J. M. *Inorg. Chim. Acta* **2009**, *362*, 4449–4460.

(44) Tangen, E.; Conradie, J.; Ghosh, A. *J. Chem. Theory Comput.* **2007**, *3*, 448–457.

(45) Wang, Y.; Espenson, J. H. *Inorg. Chem.* **2002**, *41*, 2266–2274.

(46) Jacobi, B. G.; Laitar, D. S.; Pu, L.; Wargocki, M. F.; DiPasquale, A. G.; Fortner, K. C.; Shuck, S. M.; Brown, S. N. *Inorg. Chem.* **2002**, *41*, 4815–4823.

(47) Crestoni, M. E.; Fornarini, S.; Lanucara, F.; Warren, J. J.; Mayer, J. M. *J. Am. Chem. Soc.* **2010**, *132*, 4336–4343.

(48) Brady, C.; McGarvey, J. J.; McCusker, J. K.; Toftlund, H.; Hendrickson, D. N. *Top. Curr. Chem.* **2004**, *235*, 173–184.

(49) Scepaniak, J. J.; Bontchev, R. P.; Johnson, D. L.; Smith, J. M. *Angew. Chem., Int. Ed.* **2010**, *50*, 6630–6633.

(50) Wang, W.-D.; Guzei, I. A.; Espenson, J. H. *Organometallics* **2001**, *20*, 148–156.

(51) Interestingly, as described above, nitrogen atom transfer from **3** to phosphites is slower than to PPh_3 , which we attribute to the lower σ -basicity of phosphites. This suggests that the π -basicity of the nitrido ligand is less than that of the oxo ligand in $MeRe(NAr)_2O$.

(52) Kail, B. W.; Pérez, L. M.; Zarić, S. D.; Millar, A. J.; Young, C. G.; Hall, M. B.; Basu, P. *Chem.—Eur. J.* **2006**, *12*, 7501–7509.

(53) Saouma, C. T.; Peters, J. C. *Coord. Chem. Rev.* **2011**, *255*, 920–937, and references cited therein.

(54) Hay-Motherwell, R. S.; Wilkinson, G.; Hussain-Bates, B.; Hursthouse, M. B. *Polyhedron* **1993**, *12*, 2009–2012.

(55) Cirera, J.; Ruiz, E.; Alvarez, S. *Inorg. Chem.* **2008**, *47*, 2871–2889.

(56) (a) Brown, S. D.; Peters, J. C. *J. Am. Chem. Soc.* **2005**, *127*, 1913–1923. (b) Moret, M.-C.; Peters, J. C. *Angew. Chem., Int. Ed.* **2011**, *50*, 2063–2067.

(57) Seymore, S. B.; Brown, S. N. *Inorg. Chem.* **2000**, *39*, 325–332.